

# Branching fractional Brownian motion as neuron axons

Reece Beattie-Hauser,<sup>1</sup> Jonathan House,<sup>1</sup> Gaurav Khairnar,<sup>1</sup>  
Skirmantas Janušonis,<sup>2</sup> Ralf Metzler,<sup>3</sup> and Thomas Vojta<sup>1</sup>

<sup>1</sup>*Department of Physics, Missouri University of Science & Technology, Rolla, Missouri 65409, USA*

<sup>2</sup>*Department of Psychological and Brain Sciences, University of California,  
Santa Barbara, Santa Barbara, California 93106, USA*

<sup>3</sup>*Institute of Physics and Astronomy, University of Potsdam, D-14476 Potsdam-Golm, Germany*

(Dated: April 3, 2023)

Fractional Brownian Motion (FBM) is a stochastic process with long-time correlations modeling anomalous diffusion in many systems. Recently, it has been used to model the distribution of serotonergic fibers in the brain [1, 2]. To better represent these fibers, we introduce a new process, branching FBM (bFBM), where particles perform FBM but may randomly split into two. We study subdiffusive and superdiffusive bFBM, both in free space and in bounded intervals while examining three potential behaviors of the correlations (memory) in a branching event: both particles keep the memory of previous steps, only one keeps the memory, and neither keeps the memory. We calculate particles' mean-square displacements and densities, and find that qualitative features of bFBM strongly depend on memory behavior.

## I. INTRODUCTION

The brains of all vertebrate animals are permeated by a dense network of neuron axons that release the neurotransmitter serotonin. These serotonergic axons (also called fibers) belong to cells whose bodies reside in a number of brainstem clusters known as the raphe nuclei [2]. Much is known about the impact these fibers have on the brain; for instance, perturbations to the density of this fiber network have been associated with Major Depressive Disorder and epilepsy [3, 4]. Unfortunately, very little is known about how the network develops, though the traditional view is that the fibers grow according to biological necessity. However, it has recently been suggested that the growth of these fibers is actually a stochastic process [5]. This proposal turns the traditional view of the network's development on its head: rather than the network's necessary functionality dictating its development, now the network's random development dictates its functionality.

With a deep understanding of the mechanism driving the fibers' growth still forthcoming, the question arises of how one can model the network's development. Brownian motion (BM) — a very well-understood process studied by the likes of Einstein [6] — distinguishes itself as a candidate for a model of these fibers. BM is a model for normal diffusion that describes the motion of particles suspended in a fluid as a series of random walks. In these terms, the diffusing particles experience random “kicks” from the surrounding medium that result in the particle moving about in a random path. But the description provided by BM is not exclusive to particles diffusing through a fluid. Here, the path traced out by a particle's random walk would be analogous to the shape of an individual fiber.

However, the qualitative behavior of the fibers does not match that of BM paths. BM paths are far too erratic and change direction much more frequently than

the fibers do, or one could say that the fibers appear to be “stretched-out” compared to BM paths. Imagine that BM paths are like a tangled bunch of yarn, while the fibers are like that same bunch of yarn if one tried to untangle it out by pulling on it from both ends: considerably straighter, but still tangled and bent.

Instead consider fractional Brownian motion (FBM), an extension to BM that describes a considerably broader range of systems, including the motion of polymer chains [7] and the transport of insulin between biological cells [8]. The shortcomings of BM as a model of serotonergic fibers can be alleviated in FBM. In particular, the issue of BM's overly erratic nature can be addressed in FBM, where a trajectory's tendency to change direction can be adjusted (see Sec. II for details). An example of the discovered similarity between the fibers and FBM trajectories can be seen in Fig. 1, and an in-depth evaluation of the quality FBM as a model of serotonergic fibers can be found in Ref. [2].

Though FBM has been found to function well as an approximation of the fibers, the model can still be refined. Unlike FBM trajectories, serotonergic fibers have been observed to occasionally branch (see Fig. 2) and they also eventually terminate. To better represent the real fibers, we introduce branching fractional Brownian motion (bFBM), which incorporates these behaviors into the model of FBM. Of the two behaviors, the more important is branching, because it can have an effect on the long-term behavior of the system, as will be laid out in more detail in Sec. II B.

## II. FRACTIONAL BROWNIAN MOTION

As mentioned in the introduction, FBM is an extension of BM. In BM, every step a particle (also called a walker) makes is random, which is to say that the individual steps are *uncorrelated*. This sort of motion for a collection of particles results in normal diffusion [6],

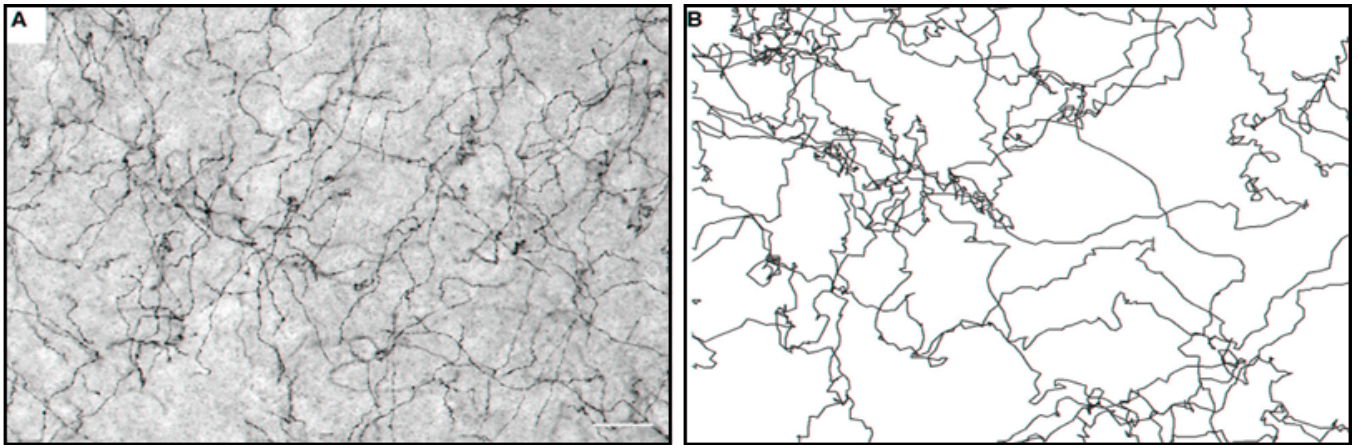


FIG. 1. Side-by-side comparison of serotonergic fibers and FBM trajectories demonstrating their similarity. Figure taken with permission from Ref. [2]. (A) 40  $\mu\text{m}$ -thick cross section of mouse brain with serotonergic fibers highlighted in black. (B) Simulated superdiffusive FBM sample trajectories ( $\alpha = 1.6$ ).

so the particles' mean squared displacement (MSD) thus follows the relationship

$$\langle x^2 \rangle \sim t \quad (1)$$

where the angle brackets denote an average over every particle in the collection and the  $\sim$  denotes proportionality.

However, if the steps a particle makes are not uncorrelated over long times — meaning a particle has *memory* of its previous steps — then the resulting motion is anomalous diffusion, where the particles' MSD now has a power of  $\alpha$ :

$$\langle x^2 \rangle \sim t^\alpha \quad (2)$$

where  $\alpha$  is the anomalous diffusion exponent, lying in the range  $0 < \alpha < 2$ . This is where we find the distinction between FBM and BM: BM is a model of *normal* diffusion, while FBM is a model of *anomalous* diffusion.

We now arrive at the two distinct types of anomalous diffusion, defined by their different values of  $\alpha$ . If a system has an anomalous diffusion exponent in  $0 < \alpha < 1$ , then the system is said to be *subdiffusive*, but if the system has  $1 < \alpha < 2$ , then it is *superdiffusive*. As their

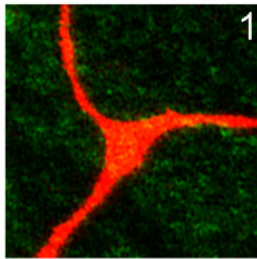


FIG. 2. Image showing the branching of a serotonergic fiber, originally published in Ref. [9]. The area pictured is about 9.5  $\mu\text{m}$  by 9.5  $\mu\text{m}$ .

names imply, the two types of anomalous diffusion are clearly defined by their relationship with normal diffusion, which corresponds to a value of  $\alpha = 1$ . This is also where FBM gets its name;  $\alpha$  has an integer value in BM but has a fractional value in FBM.

Examining Eq. 2, it is intuitively clear that higher values of  $\alpha$  result in the particles diffusing more quickly, hence the names given to each type of anomalous diffusion. Relative to normal diffusion, particles disperse more quickly in superdiffusion and less quickly in subdiffusion. This result has been presented without proof, and while a full derivation would be inappropriate here, we will still give a brief qualitative argument justifying it. As stated in Ref. [1], if one treats a random walk in FBM as a sequence of discrete steps (the details of which can be found in Ref. [10]), then the correlation between two different steps in a walk has the form

$$\langle \xi_n \xi_{n+m} \rangle \sim \alpha(\alpha - 1) |m|^{\alpha-2} \quad (3)$$

where  $\xi_n$  is the distance moved on the  $n$ th time step and  $\xi_{n+m}$  is the distance moved in the step  $m$  time steps later. Note that while this paper is only concerned with FBM in one space dimension, the theoretical framework being outlined can be extended to higher dimensions in a fairly straightforward manner [11, 12].

This relationship defined in Eq. 3 implies two important facts about FBM. The first is that the individual steps in a walk are negatively correlated with one another in subdiffusion but positively correlated in superdiffusion. This means a particle is less likely to move in the same direction repeatedly in subdiffusion, but would be more likely to move in the same direction in superdiffusion. As a result, lower values of  $\alpha$  cause the particles to be more likely to turn around, and so they disperse much more slowly — which is the origin of the power of  $\alpha$  in Eq. 2.

The second important fact gleaned from Eq. 3 is that the correlations between steps decay over time, but they do so relatively slowly. If the correlations decayed expo-

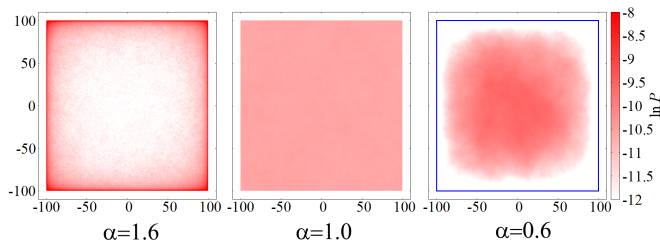


FIG. 3. Stationary probability density  $P$  of two-dimensional FBM in a square interval for superdiffusion (left,  $\alpha = 1.6$ ), normal diffusion (middle,  $\alpha = 1.0$ ), and subdiffusion (right,  $\alpha = 0.6$ ). Originally published in Ref. [1].

nentially, the behavior would revert to BM. But since the correlations decay slowly, a particle retains its “memory” of previous steps for a very long time.

### A. Success of FBM in modelling fiber densities

In the introductory section, the argument for FBM’s quality as a model of the fibers was based on the visual resemblance between the fibers and FBM paths, which is admittedly superficial. However, the evidence in favor of FBM is deeper than that, as FBM particle densities<sup>1</sup> have demonstrated a good ability to approximate the densities of the real serotonergic fibers [2].

The relative densities of FBM particles across space evolve over time. At first, the particles are all concentrated at the origin, but then they begin moving outward and their density starts to spread out, and they will continue to disperse forever, never reaching equilibrium. However, if the particles are confined inside some boundary, then eventually their density will reach a steady state and become stationary. In the case of BM (normal diffusion), this stationary density is a uniform distribution over the entire interval. However, in anomalous diffusion, the stationary density features either an accumulation near the boundary (in superdiffusion) or a depletion near the boundary (in subdiffusion) [13] (see Fig. 3 for examples).

Of particular note is the accumulation effect present in superdiffusion, as similar behavior can be seen in the densities of serotonergic fibers. Simulations of superdiffusive FBM inside a brain-like geometry have yielded results greatly resembling those of the fibers, which can be seen in Fig. 4. While the similarity may again seem to be superficial, it has actually been subjected to significant scrutiny and quantitative analysis which have indicated the already mentioned conclusion that superdif-

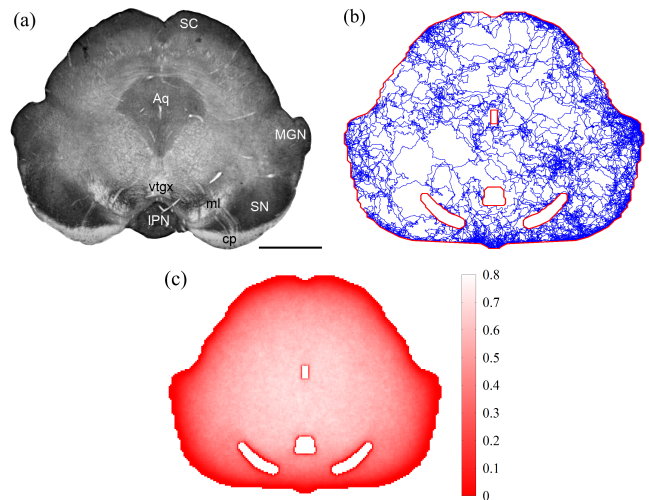


FIG. 4. Comparison of fiber densities and superdiffusive FBM probability densities. Originally published in Ref. [1]. (a) Cross section of mouse midbrain stained to highlight fiber density, with darker color indicating higher density. (b) Single simulated FBM trajectory with  $2^{17}$  steps and  $\alpha = 1.6$ . (c) Particle density of simulated FBM with  $\alpha = 1.6$  after  $2^{23}$  steps. The color scale follows  $\exp(-\beta P)$ , where  $\beta = 38000$  and  $P$  is the unmodified particle density.

fusive FBM serves as a good model for the densities of serotonergic fibers.

### B. Branching fractional Brownian motion

Though FBM has demonstrated its value in estimating the densities of serotonergic fibers, the model remains imperfect. For instance, FBM paths are infinitely long — there is no mechanism in place that would cause an FBM particle to stop moving. Perhaps more importantly, FBM paths lack a major geometric feature of serotonergic fibers: branching [9]. There is no structure or framework present in FBM that would cause or allow a particle to split into two, so to address this, we must make additions to the existing model. We call the resulting model branching fractional Brownian motion (bFBM).

In bFBM, the particles (referred to as walkers) perform FBM as normal, but on every time step there is a finite chance that a walker will branch (with probability  $\lambda_b$ ) and/or decay/terminate (with probability  $\lambda_d$ ). While introducing walker death should not have any serious effect on the qualitative features of the model, the introduction of branching walkers does conflict with the existing model of FBM (despite the simplicity of this method for modeling branching), namely in how a walker’s memory behaves at a branching event. As discussed in the main body of Sec. II, destroying a walker’s memory causes it to revert to normal diffusion, so the memory behavior at a branching event could have pronounced effects on a system’s qualitative characteristics.

<sup>1</sup> The terms particle density and probability density are used interchangeably here because the two quantities are effectively equivalent; they differ only by some constant factor depending on the chosen units.

There are two essential questions about memory behavior that must be addressed. What happens to a walker's memory when it branches? Does the new walker keep the memory of the original? While there are countless different possible answers to these two questions, here we will be studying the three simplest cases: first is that both the original walker and new walker keep the full memory of the original walker (this will be referred to as the BOTH memory model), second is that the original walker keeps its memory while the new walker must start anew (this is the ORIG memory model), and third is that neither the original or new walkers keep the memory and they must both start anew (this is the NONE memory model).

Of particular interest are the ORIG and NONE models because they cause walkers to lose memory. As just mentioned, losing memory causes the system to cross over from FBM to normal BM, an effect that has been previously studied in the context of tempered FBM [14]. However, unlike with tempered FBM, bFBM loses memory in a more "organic" fashion, as opposed to the somewhat arbitrary cutoff of correlations of tempered FBM.

### III. COMPUTER SIMULATIONS

To test our 1D discrete-time bFBM model, we ran Monte Carlo simulations of  $5 \cdot 10^3$  to  $1.2 \cdot 10^4$  initial walkers which were allowed to walk up to  $2^{13}$  or  $2^{14}$  time steps, starting from the origin. In this paper, we present our results for four different anomalous diffusion exponents,  $\alpha = 0.7$  and  $\alpha = 0.8$  for subdiffusion and  $\alpha = 1.6$  and  $\alpha = 1.8$  for superdiffusion.

For the branching and decay rates, we choose  $\lambda_b = 0.01$  and  $\lambda_d = 0.0097$ . We note that these rates are particularly close in value and that  $\lambda_b > \lambda_d$ . The two rates were chosen to be close together in order to mitigate the effect of an exponentially increasing number of walkers due to the branching. We also wanted to avoid  $\lambda_b < \lambda_d$  because it would cause the walker number will drop rapidly, as walkers would decay more quickly than they branch. This is unwanted in our study as it will result in walkers have very limited lifetimes to demonstrate their behaviors. Similarly, when  $\lambda_b = \lambda_d$ , we expect the final number of walkers to be close to the initial amount, which is also not ideal for studying branching effects. Therefore, we find that a difference of rates  $\lambda_b - \lambda_d = 0.0003$ , where the magnitudes of  $\lambda_b$  and  $\lambda_d$  were chosen arbitrarily, was sufficient for studying bFBM using our simulation.

In bounded random walks, walkers are restricted to the finite interval of  $(-L/2, L/2)$  where  $L$  is selected based on  $\alpha$  and  $\lambda_b$ . For each system, we choose  $L$  so that all three regimes for the MSD are clearly visible, the three regimes being: behaving like normal FBM, before the crossover to BM; after the crossover to BM; and after the system has reached the boundary and the MSD has saturated.

In simulating our bFBM model, long simulation times become a serious challenge. Unlike in related literature

where Fourier-filtering techniques may be used to generate fractional noise — significantly reducing simulation time and allowing the study of much longer times [1, 13] — no method was found that extended Fourier-filtering to include memory loss in branching events. Instead, we use Hosking's algorithm [15] to generate the walkers' steps for the simulation. Similar to other methods, this involves first producing uncorrelated Gaussian random numbers. We achieve this by performing a Box-Muller transformation on random numbers generated from Marsaglia's 2005 KISS random number generator [16]. Unfortunately, the Hosking method has the downside that its complexity is  $O(t^2)$ , which causes significant slowdown when simulating to longer times.

## IV. RESULTS

### A. Mean squared displacement

First we observe the unbounded MSD  $\langle x^2 \rangle$  of the walkers. Figure 5 shows the simulation results for two anomalous diffusion coefficients,  $\alpha = 0.8$  and  $\alpha = 1.6$ , with one curve for each memory model. We notice that unlike the other two models, the BOTH cases follow the same  $t^\alpha$  behavior from normal FBM, as expected. Just as in FBM, there is no mechanism by which a walker can lose its memory since branched walkers keep the exact memory as the walker from which they originated.

In the other two models, NONE and ORIG, the resulting curves illustrate a break from this FBM  $t^\alpha$  behavior, showing a distinct crossover point at  $t \approx 100$ . This crossover is a consequence of our ORIG and NONE memory models introducing memory loss during branching events. Prior to the crossover time, walkers follow the FBM behavior associated with their corresponding  $\alpha$ . However after this crossover point, walkers without memory begin to dominate the system. This domination of walkers without memory causes our system to cross over and begin to diffuse linearly like normal BM ( $\alpha = 1$ ).

The reason for the crossover occurring at  $t \approx 100$  is also easily explained. Note that  $1/\lambda_b = 100$ . This means that on average, we expect 100 time steps to pass before we reach our first branching event, so we expect on average 100 time steps to pass before a new walker with no memory is created (in the ORIG model) or a walker's memory is lost altogether (in the NONE model). The memory loss is what causes this crossover to BM, so it is expected that the crossover becomes visible in the MSD around  $t \approx 100$ .

Looking closely at the curves for the ORIG and NONE memory models in Fig. 5, we see the crossover to BM happens more quickly in the case where none of the walkers keep the memory of the original walker. This makes intuitive sense, as the system as a whole loses memory more quickly when the individual walkers lose their memory when they branch, rather than the original still keeping

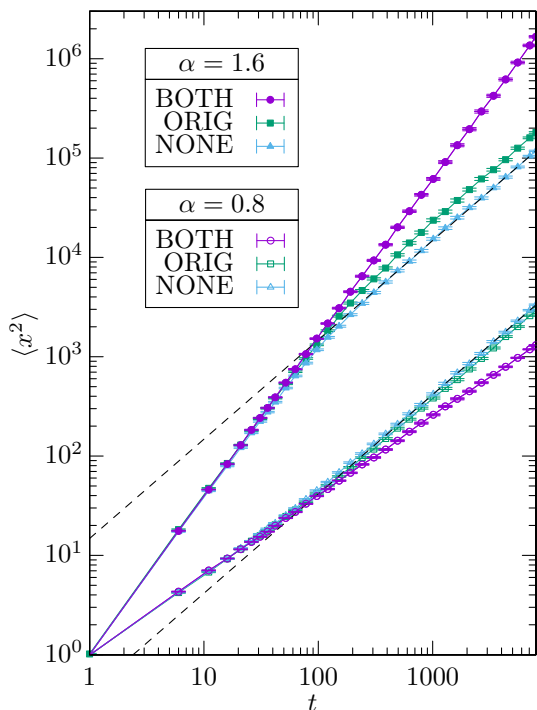


FIG. 5. The mean squared displacement as a function of time for  $1.2 \cdot 10^4$  initial walkers, simulated up to 8000 time steps inside an infinite interval. Data is plotted on a double-logarithmic scale. Dotted lines show the post-crossover BM-like behavior ( $\alpha = 1$ ) for the NONE curves.

its memory. This effect is noticeable when comparing the simulation curves produced by these models. In our superdiffusive case ( $\alpha = 1.6$ ), we notice that after the crossover point, the ORIG model begins to take on a larger  $\langle x^2 \rangle$  than the NONE model. As explained, this is because the crossover from the  $t^\alpha$  FBM behavior into the linear BM behavior happens more slowly for the ORIG model than it does for the NONE model. Similarly, in the subdiffusive case ( $\alpha = 0.8$ ), we notice that the ORIG model begins to take on smaller  $\langle x^2 \rangle$  than the NONE model after the crossover point.

Next we observe the bounded MSD  $\langle x^2 \rangle$  of the walkers. Figure 6 shows the simulation results using two different  $\alpha$  with one curve for each of our memory models. We now notice a new region in our curves where the system reaches the boundary of the interval and the mean squared displacement saturates. One observation about the saturation value of  $\langle x^2 \rangle$  is that it differs across both values of  $\alpha$  and memory model.

Take note of the difference in the saturated MSD between the different memory models in the subdiffusive case. We notice that the NONE and ORIG cases saturate to similar values, both greater than that of the BOTH case — despite the BOTH model having a significantly larger interval length. In normal FBM, we would expect the system with the greater  $L$  to have the greater saturated MSD. However, the saturation value of the MSD

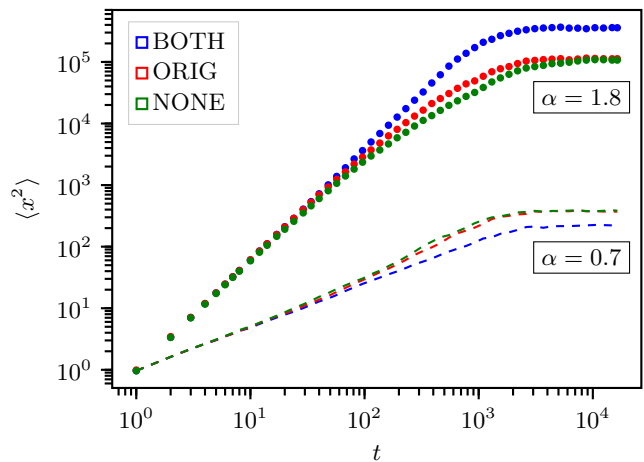


FIG. 6. The mean squared displacement as a function time for  $5 \cdot 10^3$  initial walkers, simulated up to  $2^{14}$  time steps inside a finite interval. The upper, circle marked curves correspond to  $\alpha = 1.8$  and the lower, dashed line curves to  $\alpha = 0.7$ . The interval length used for  $\alpha = 1.8$  was  $L = 1400$  (for the BOTH model) and  $L = 1061$  (for the ORIG and NONE models). The interval length used for  $\alpha = 0.7$  was  $L = 64$  (for BOTH) and  $L = 35$  (for ORIG and NONE). Data is plotted on a double-logarithmic scale.

depends on both  $L$  and  $\alpha$ , as studied in Ref. [17]. This means that the ORIG and NONE models, which both have an effective anomalous diffusion exponent of  $\alpha = 1$  after the crossover, will have a much greater saturated MSD than BOTH, which has  $\alpha = 0.7$ , despite BOTH having a greater interval  $L$ .

## B. Probability densities

Figures 7 and 8 show the steady-state probability densities for  $\alpha = 1.8$  and  $\alpha = 0.7$ , respectively, again with one curve for each of the three memory models.

First we observe the BOTH memory case in each figure. Note the steep increases and decreases towards the edges of the plots, which is the accumulation or depletion of walkers at the interval boundaries. This behavior is identical to that of normal FBM [1]. By the same argument used in Sec. IV A, this behavior is expected because of the equivalency between the BOTH memory model and normal FBM.

Compare this result to the ORIG and NONE memory models, whose probability densities are much flatter in the middle than those for the BOTH model. This behavior is similar to that of BM, where the probability density would be completely flat and uniform in a steady state. By the same arguments as those made in Sec. IV A, this similarity is due to the crossover to BM caused by the systems being dominated by walkers that have no memory.

However, the distributions for these memory-losing models are not completely uniform like those of BM,

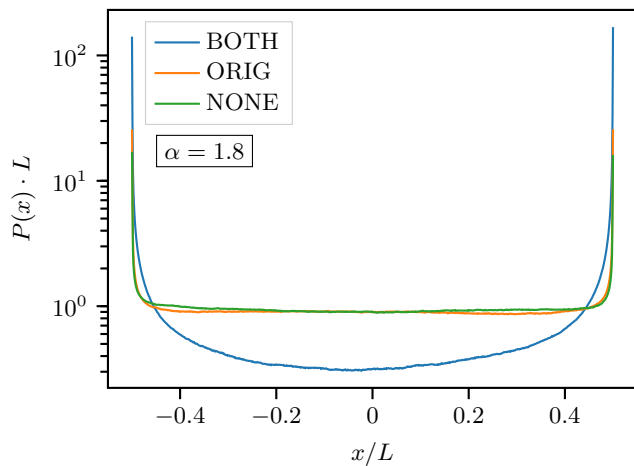


FIG. 7. The scaled probability distributions  $PL$  plotted against  $x/L$  for all three memory models in the superdiffusive case ( $\alpha = 1.8$ ). The distribution is averaged over  $5 \cdot 10^3$  initial walkers after being simulated for  $2^{14}$  time steps.

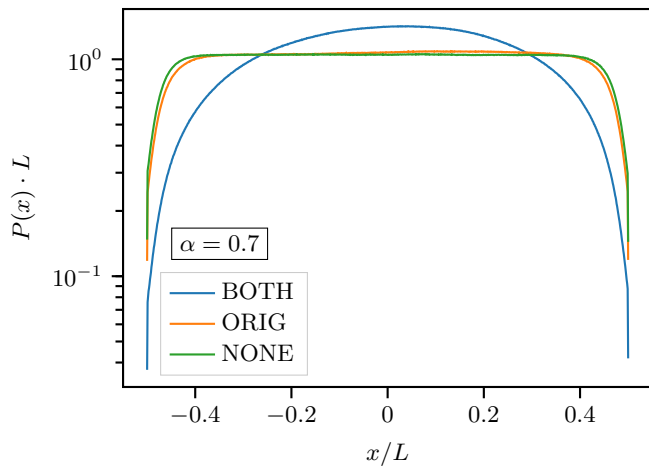


FIG. 8. The scaled probability distributions  $PL$  plotted against  $x/L$  for all three memory models in the superdiffusive case ( $\alpha = 1.8$ ). The distribution is averaged over  $5 \cdot 10^3$  initial walkers after being simulated for  $2^{14}$  time steps.

as there are still accumulation (for superdiffusion) and depletion (for subdiffusion) near the boundaries of the interval, somewhat similar to those of FBM. But unlike FBM, these accumulation and depletion effects are restricted to narrow region at each boundary, whereas in the BOTH model, these effects are over the entire interval — seen in how its distribution is never completely flat like the distributions for the ORIG and NONE models. Additionally, we note that the restricted accumulation and depletion in the memory-losing models is similar to in distributions produced by tempered FBM [14].

Again similar to the results found in Sec. IV A, there is a slight visible difference between the ORIG and NONE curves. In Fig. 7, we observe the distribution for the

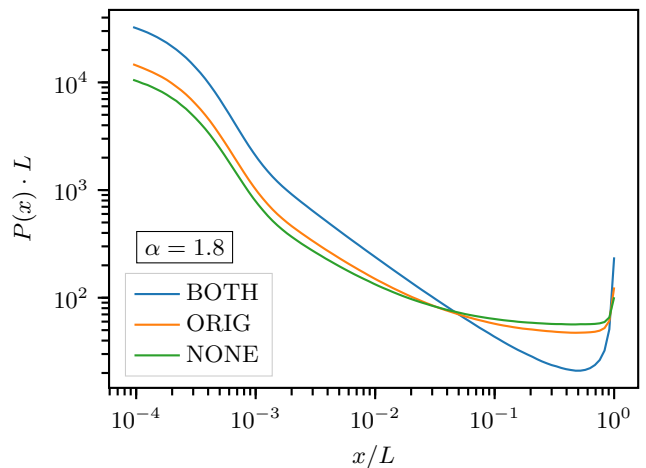


FIG. 9. The scaled probability distributions  $PL$  plotted against  $x/L$  on a double-logarithmic scale for all three memory models in the superdiffusive case ( $\alpha = 1.8$ ), where  $x$  is now the distance from the edge of the boundary. The distribution is averaged over  $5 \cdot 10^3$  initial walkers after being simulated for  $2^{14}$  time steps.

NONE model in superdiffusion to be slightly higher in the middle region than the distribution for the ORIG model. This result agrees with the other results already outlined, as it indicates that the behavior in the NONE model is slightly more similar to normal BM than the ORIG model. This is because walkers in the NONE model tend to retain their memory for a shorter period of time than in the ORIG model.

Similarly, for the subdiffusive systems shown in Fig. 8, we observe the probability density for the ORIG model to be slightly higher in the center of the interval than in the NONE model. This is for a similar reason as in the superdiffusive case, only inverted: the ORIG model keeps memory for slightly longer than the NONE model, so the depletion effect is slightly stronger in the ORIG model. As a result, it is slightly more likely for a walker to be in the center of the interval rather than at the boundary in the ORIG model.

Let us also examine the probability densities plotted on a double-logarithmic scale, as seen in Fig. 9. Note that We now track each walker's distance from the wall at the edge of the finite interval instead of the distance from the origin. Since this distribution is for the superdiffusive case, we observe that the distribution closer to the wall features an accumulation of walkers. Due to this simulation of walkers being on a finite interval, this accumulation effect saturates as we enter  $x/L < 10^{-3}$ .

Most interestingly, however, is how the ORIG and NONE cases seem to approach the behavior of the BOTH case. Notice first the region in the BOTH case before saturation where the distribution's slope is relatively constant, which indicates that the FBM correlations are present along the entire interval. Conversely, along this same interval, the memory loss models do not

have this constant slope. Past the point where the NONE and ORIG distributions intersect the BOTH distribution, there is a flat region in the models with memory loss, caused by the BM behavior of these models. However, as previously discussed, we expect the regions towards the ends of the intervals to display FBM correlations. We note that in regions closer to the wall but before before saturation, the slopes of the distributions for the memory loss models are very similar to the slope of the distribution for the BOTH model. This behavior agrees with our expectation that the memory loss models contain a somewhat stronger concentration of walkers that still have their memory in this region.

## V. DISCUSSION

To summarize, we introduce bFBM, an extension of FBM in which paths can now spontaneously branch apart or terminate. To this end, we propose three memory models, which we call BOTH, ORIG, and NONE. In our preliminary results, we find a qualitative agreement with our expectations for each model, namely that the BOTH model reproduces normal FBM while the ORIG and NONE models cross over to normal BM as a result of their loss of memory. The BOTH model recovering the behavior of FBM (particularly the accumulation effect of superdiffusion) is an important result, as it reinforces the validity of previous works that found success with normal FBM as a model of serotonergic fibers [1, 2], despite neglecting the fibers' branching behavior.

As previously noted, further exploration into the relationship between tempered FBM [14] and the memory loss of the ORIG and NONE may be warranted, as both exponentially tempered FBM and strong power-law tempered FBM also contain crossovers to normal BM. This agrees with intuition, since both bFBM and tempered FBM interrupt walker correlations: tempered FBM cuts off correlations with exponential or power-law mechanisms, while bFBM cuts off correlations through branching and decay mechanisms. Additionally, we find qualitative similarities in the steady-state distributions of exponentially tempered FBM and strong power-law tempered FBM and bFBM. We find that both models' distributions share FBM accumulation and depletion ef-

fects in narrow regions near the walls of their interval. Likewise, the log-log steady-state distributions of tempered FBM and bFBM both seem to approach normal FBM.

To close, we return to the application of the bFBM model in the representation of serotonergic fibers. The introduction of bFBM, which now reflects the fibers' branching and decay behaviors, shows potential as an improvement of the model of this biological system. However, there is still quantitative analysis comparing these systems that needs to be done, but unfortunately, this will require gathering more biological data to compare to. For example, recall that the values of both the branching rate  $\lambda_b$  and decay rate  $\lambda_d$  were chosen arbitrarily. Data corresponding to rates for these fibers, such as their magnitudes or relative difference, has yet to be collected. Once that information is obtained, though, we will be ready to continue the work we have started here.

## ACKNOWLEDGMENTS

Reece would like to thank Dr. Thomas Vojta for his sage advice and seemingly limitless patience. Reece isn't sure if it was Dr. Vojta, Dr. Skirmantas Janušonis, or Dr. Ralf Metzler who first suggested that the three of them collaborate on serotonergic fiber research, but he would like to thank them for the opportunity they've inadvertently given him in their collaboration. And of course he would thank Dr. Vojta for choosing to give him this opportunity.

Reece would also like to thank Gaurav Khairnar for his help with improving the implementation of the Hosking algorithm in the simulation, as well as for other general guidance he has given.

Jonathan would like to thank Dr. Thomas Vojta for all the time and help he's graciously given throughout this research. Without his support and expertise, this certainly would not have been possible. Jonathan would also like to thank Reece for all his help with writing and revising this paper.

This work was supported in part by the National Science Foundation under Grant No. IIS-2112862 and by the Cottrell SEED award from Research Corporation.

- 
- [1] T. Vojta, S. Halladay, S. Skinner, S. Janušonis, T. Guggenberger, and R. Metzler, *Phys. Rev. E* **102**, 032108 (2020).
  - [2] S. Janušonis, N. Detering, R. Metzler, and T. Vojta, *Front. Comput. Neurosci.* **14**, 56 (2020).
  - [3] Y. Numasawa, T. Hattori, S. Ishiai, Z. Kobayashi, T. Kamata, M. Kotera, S. Ishibashi, N. Sanjo, H. Mizusawa, and T. Yokota, *J. Affect. Disord.* **213**, 191 (2017).
  - [4] G. H. Maia, J. I. Soares, S. G. Almeida, J. M. Leite, H. X. Baptista, A. N. Lukoyanova, C. S. Brazete, and N. V. Lukoyanov, *Brain Res. Bull.* **152**, 95 (2019).
  - [5] S. Janušonis and N. Detering, *Biochimie* **161**, 15 (2019).
  - [6] A. Einstein, *Investigations on the Theory of the Brownian Movement* (Dover, 1956).
  - [7] N. Chakravarti and K. Sebastian, *Chem. Phys. Lett.* **267**, 9 (1997).
  - [8] S. M. A. Tabei, S. Burov, H. Y. Kim, A. Kuznetsov, T. Huynh, J. Jureller, L. H. Philipson, A. R. Dinner, and N. F. Scherer, *Proc. Natl. Acad. Sci. USA* **110**, 4911 (2013).

- [9] M. Hingorani, A. Viviani, J. Sanfilippo, and S. Janušonis, *Front. Neurosci.* **16**, 994735 (2022).
- [10] H. Qian, in *Processes with Long-Range Correlations*, Lecture Notes in Physics, Vol. 621, edited by G. Rangaran and M. Ding (Springer, 2003) p. 22.
- [11] H. Qian, G. M. Raymond, and J. B. Basingthwaight, *J. Phys. A: Math. Gen.* **31**, L527 (1998).
- [12] R. Metzler and J. Klafter, *J. Phys. A: Math. Gen.* **37**, R161 (2004).
- [13] A. H. O. Wada and T. Vojta, *Phys. Rev. E* **97**, 020102 (2018).
- [14] T. Vojta, Z. Miller, and S. Halladay, *Eur. Phys. J. B* **94**, 208 (2021).
- [15] J. R. M. Hosking, *Water Resource Research* **20**, 1898 (1984).
- [16] G. Marsaglia, "Double precision RNGs", posted to sci.math.num-analysis (2005).
- [17] T. Guggenberger, G. Pagnini, T. Vojta, and R. Metzler, *New J. Phys.* **21**, 022002 (2019).